

NATIONAL INSTITUTE FOR FUSION SCIENCE

Observation of Plasma Toroidal Rotations Driven by the Electric Field due to a Loss of Ions

K. Ida, K. Kawahata, K. Toi, T. Watari, O. Kaneko, Y. Ogawa, H. Sanuki, K. Adati,
R. Akiyama, A. Ando, R. Ando, Y. Hamada, S. Hidekuma, S. Hirokura, A. Karita,
T. Kawamoto, Y. Kawasumi, M. Kojima, R. Kumazawa, T. Kuroda, K. Masai,
S. Morita, K. Narihara, K. Ohkubo, Y. Oka, S. Okajima, T. Ozaki, M. Sakamoto,
M. Sasao, K. Sato, K.N. Sato, T. Seki, F. Shimpo, Y. Taniguchi, T. Tsuzuki,
and H. Yamada

(Received - Jan. 30, 1990)

NIFS-23

Mar. 1990

RESEARCH REPORT NIFS Series

This report was prepared as a preprint of work performed as a collaboration research of the National Institute for Fusion Science (NIFS) of Japan. This document is intended for information only and for future publication in a journal after some rearrangements of its contents.

Inquiries about copyright and reproduction should be addressed to the Research Information Center, National Institute for Fusion Science, Nagoya 464-01, Japan.

NAGOYA, JAPAN

Observation of plasma toroidal rotations driven
by the electric field due to a loss of ions

K.Ida, K.Kawahata, K.Toi, T.Watari, O.Kaneko, Y.Ogawa, H.Sanuki,
K.Adati, R.Akiyama, A.Ando, R.Ando, Y.Hamada, S.Hidekuma,
S.Hirokura, A.Karita, T.Kawamoto, Y.Kawasumi, M.Kojima,
R.Kumazawa, T.Kuroda, K.Masai, S.Morita, K.Narihara, K.Ohkubo,
Y.Oka, S.Okajima, T.Ozaki, M.Sakamoto, M.Sasao, K.Sato, K.N.Sato,
T.Seki, F.Shimpo, Y.Taniguchi, T.Tsuzuki, and H.Yamada

National Institute for Fusion Science, Nagoya 464-01, Japan

Abstract

Plasma toroidal rotations not driven by the momentum input but by the electric field due to a loss of ions have been observed for the plasmas heated with perpendicular neutral beam injection. They are found to be increased in the counter direction to the plasma current as plasma ions are heated with ion cyclotron resonance frequency waves. The electric field derived from rotations are quantitatively consistent with those inferred from the ambipolarity of particle fluxes.

'keywords' plasma rotation, electric field, ambipolar flux, momentum balance, tokamak plasma

Recent theories predict that the plasma electric field and space potential play an important role in a transition from low confinement (L-mode) to high confinement (H-mode) plasmas and/or improved ohmic confinement (IOC) plasmas¹⁻³⁾. Experimental observations show that the toroidal rotations correlate to the plasma confinement. Improvement of impurity particle and energy confinement have been observed with counter neutral beam injection (NBI) experiments in ISX-B⁴⁾ and ASDEX⁵⁾, respectively. Reduction of ion and electron heating has been reported in the TFTR plasma which has a strong rotation.⁶⁾ These theories and experiments show that the both electric field and toroidal rotation have strong effects on the improvement of the plasma confinement. Direct measurements of the space potential distribution have been done for NBI plasmas in ISX-B and ohmic plasmas in TM-4 tokamak, using beam probe methods⁷⁻⁹⁾. The electric fields have been derived indirectly from plasma rotation measurements in stellarator/heliotron plasmas using a radial momentum balance equation^{10,11)}.

Most toroidal rotation measurements have been done for the plasma heated by tangentially injected neutral beams to study the angular momentum confinement.^{12,13)} In these analysis only the direct momentum input from injected beams are taken into account, since the toroidal rotations due to electric field are smaller than that due to the momentum of NBI. However the toroidal rotations induced by the electric field become significant for the plasma heated by perpendicular NBI. In this paper, we present the toroidal rotations not due to the direct momentum of NBI but due to the radial electric field induced by a loss of ions. Parameter dependence of the space potentials given by integrating the

radial electric field are also described.

The radial momentum balance equation yields the radial electric field from which the potential Φ is calculated. The momentum due to this potential should be balanced to the others caused by the ion pressure gradient ∇p_i , the toroidal rotation $V_\phi B_\theta$, and the poloidal rotation $V_\theta B_r$. In tokamak plasmas especially with low aspect ratio, the pressure gradient and toroidal rotation are the dominant terms, since the poloidal rotation is small due to the large viscosity associated with toroidal effect.¹⁴⁻¹⁶⁾ Poloidal rotation velocities 3 ~ 5 cm inside the plasma are measured with intrinsic CIV line radiation without neutral beam. They are found to be smaller than the minimum detectable rotation velocity of our spectroscopy system (~ 2 km/s) for our experiment. An electric field ($-\partial\Phi/\partial r$) can be derived from the measured toroidal rotation velocity V_ϕ and the ion pressure gradient using radial momentum balance equation,

$$eV_\phi B_\theta = -T_i \left(\frac{\partial \ln p_i}{\partial r} - (\beta, g) \frac{\partial \ln T_i}{\partial r} + \frac{e}{T_i} \frac{\partial \Phi}{\partial r} \right), \quad (1)$$

where (β, g) is a numerical coefficients depending on the collisionality regime¹⁷⁾. In JIPP TII-U both toroidal rotation velocity and ion temperature profile are measured with a multi-chord spectrograph using the charge exchange recombination spectroscopy¹⁸⁾.

The radial profiles of the toroidal rotation velocity, ion temperature and electron density for a 0.7 MW perpendicular NBI discharge and for a 0.7 MW NBI plus 1.4 MW ion cyclotron resonance frequency (ICRF) heated discharge are shown in Figs. 1(a)-(c). The plasma rotates in the

direction opposite of the plasma current (counter-direction) during NBI (slightly tilted to co-direction). The plasma rotation profile is hollow and it is significantly different from that observed in the plasma heated with tangential neutral beams. The direction and the profile of the toroidal rotation velocity can not explained with the momentum input of neutral beam injection. This speed increases as the ion temperature increased by applying ICRF waves.¹⁹⁾ The radial electric field profile is peaked at a radius of $r = (2/3)a$, as shown in Fig. 2(a), where a is the plasma minor radius. The peak values are -130 V/cm for NBI and -210 V/cm for NBI plus ICRF heated plasmas, respectively. Other measurements related with the electric field shows the consistent results. The dispersion relations of the drift waves-type density fluctuations have been measured with HCN laser scattering²⁰⁾, and the electric field is estimated to be -90 V/cm at $r = 16$ cm (corresponding to $R = 107$ cm) assuming the measured phase velocity is the superposition of the electron diamagnetic drift velocity on Doppler shifts. The electric field near the plasma center ($r = 3$ cm, $R = 94$ cm) is estimated by using $m/n=1/1$ MHD oscillations and found to be -20 V/cm (NBI) - 40 V/cm (NBI+ICRF).

The negative potential derived by integrating the radial electric field along the minor radius becomes deeper with NBI+ICRF combined heating than with only NBI heating, as shown in Fig.2(b). In order to investigate its parameter dependence, a parameter scan was performed with various electron densities and plasma currents for NBI and ICRF heated plasmas. The plasma space potentials depends most strongly on the ion temperature, and these values are 1.5 times the central value of the ion temperature for both NBI and ICRF heated plasmas, as shown in Fig.3. No significant

dependence of the space potential on the electron temperature and density and plasma current is observed. The beam line of NBI is tilted typically in co-direction (a direction of plasma current) only by 9 degree. The direction of the plasma current was reversed to check the effect of the momentum input of NBI on the space potential. No change of direction of the toroidal rotation velocity, however, the momentum input of the neutral beam changes space potentials slightly as demonstrated in Fig.3.

Nonambipolar fluxes should exist in the plasma, since the negative plasma potentials are obtained. Nonambipolar direct ion loss has a important role only in the region of $|a-r| < \rho_p$ ¹⁾, where ρ_p is poloidal gyroradius, however it should be negligible in the plasma core. The nonambipolar ion particle flux induced by the plasma momentum loss associated with charge exchange processes should be taken into account especially in the plasma periphery²⁾. However, this flux can be neglected in the core region, where the neutral density is below 10^8 cm^{-3} for the plasma rotating toroidally at the velocity of $20 \sim 30 \text{ km/s}$. According to the neoclassical ripple transport theory^{21,22)} there is a finite residual toroidal rotation velocity due to toroidal field ripples in the banana regime and the electric field predicted to be

$$eE = \frac{T_i}{n_e} \frac{\partial n_e}{\partial r} + \alpha_{neo} \frac{\partial T_i}{\partial r}, \quad (2)$$

where α_{neo} is a function of the ripple depth and collision frequency and in the range of $2.5 \sim 3.5$. The predicted electric field is much larger than the measured values as shown with dashed lines in Fig. 2 and 3. The central space potential given by integrating this electric field is about

four times of the central ion temperature and larger than the measured values by a factor of $2 \sim 3$.

Here we will take a simple model using the Einstein relations between diffusion and mobility, to explain the measured electric field and potentials. An inward pinch term is added only in the electron flux to produce the negative potential. The ion and electron radial fluxes in the plasma core can be modeled by,

$$\Gamma_e = -D_e \left(\frac{\partial n_e}{\partial r} + \frac{\alpha_e n_e}{T_e} \frac{\partial T_e}{\partial r} + \frac{n_e e E}{T_e} \right) - v_{pinch}, \quad (3)$$

$$\Gamma_i = -D_i \left(\frac{\partial n_i}{\partial r} + \frac{\alpha_i n_i}{T_i} \frac{\partial T_i}{\partial r} - \frac{n_i e E}{T_i} \right), \quad (4)$$

where D_e and D_i are the electron and ion anomalous diffusion coefficients, and α_e and α_i are numerical coefficient of order unity and v_{pinch} is nonambipolar pinch term. Eq.(3) is divided to diffusive and convective terms as $\Gamma_a = -D_e(r) \partial n_e / \partial r + v(r) n_e$. Radial dependences of $D_e(r) = D(0) / (n_e(r) / n_e(0))$ and $v(r) = v_a (r/a)^3$ are introduced to fit the measured electron density profiles. The values $D(0)$ and v_a are measured to be $0.5 \text{ m}^2/\text{s}$ and -40 m/s (inward) in the small ice pellet injection experiment.²³⁾ The absolute values of these coefficient have error in the measurement by factor of two due to that the change of electron density profile by ice pellet is too small to specify more accurate values. However, the ratio of convective velocity to diffusion is measured with 10 - 20 % error, since this ratio is only determined by the electron density

profile in steady state. Since the Z_{eff} is $2 \sim 2.5$ and $n_e \sim n_i$ for these discharges²⁴⁾, the ambipolar electric field for $\Gamma_i = \Gamma_e$ can be shown as

$$eE = \frac{D_i - D_e}{D_i} \frac{T_i}{n_e} \frac{\partial n_e}{\partial r} + \frac{\alpha_i \delta T_i}{\partial r} + \frac{v}{D_i} T_i. \quad (5)$$

The estimated electric field and space potential assuming $D_e = D_i$ are also shown with solid lines in Fig.2. The electric field and space potential radial distribution estimated from ambipolarity of particle fluxes shows reasonable agreement with the measured data points from plasma rotation velocity distribution.

By integrating Eq.(5), the space potential between plasma center and plasma edge is obtained as follows,

$$\Phi(a) - \Phi(0) = \left(\frac{D_i - D_e}{\eta_i D_i} + \alpha_i + \frac{\bar{c}_v D_e}{s D_i} \right) \frac{T_i}{e}, \quad (6)$$

where η_i and α_i is the ratio of the gradient of ion temperature to that of the electron density and a numerical coefficient of ~ 1 . The value of η_i is $1.0 \sim 1.2$ for the present experiment. The peaking parameter $c_v = -v(r) a^2 / (2r D_e(r))$ is relatively constant in space. The parameter $s = T_i(0) / \langle T_i \rangle$, where $\langle \rangle$ represents a volume averaged, and line averaged peaking parameter \bar{c}_v are factors derived from the shape of ion temperature and electron density, and $s \sim 2.7$ and $\bar{c}_v \sim 1.5$. The estimated space potential derived from ambipolarity for $D_i = D_e$ is shown by a solid line in Fig.3. This estimation agrees well with the measured ratio of the central space potential to the central ion temperature.

The nonambipolar fluxes are induced by toroidal field ripples, fast ion orbit loss, charge exchange loss and electron pinch velocity. The electric field and potential estimated by toroidal field ripples are larger than the measured values by factor of more than two. The observation of intrinsic toroidal rotations can not be explained by neoclassical nonambipolar fluxes alone. It is still open to question which loss is most dominant in the plasma, however it is clear that the plasmas have negative potential and toroidal rotations due to this electric field without any direct momentum input. This intrinsic toroidal rotations is important to study the momentum confinement.

The authors wish to thank K.Itoh and S.-I.Itoh for useful discussions.

Reference

¹S.-I.Itoh and K.Itoh, Phys. Rev. Lett. 60 (1988) 2276.

²K.C.Shaing, et al., in Plasma Physics and Controlled Nuclear Fusion Research (Proc. 12th Int. Conf., Nice, 1988) IAEA-CN-50/D-I-2.

³S.-I.Itoh and K.Itoh, Research Report HIFT-163 (Hiroshima Inst. for Fusion Theory 1989)

⁴R.C.Isler et al., Phys. Rev. Lett. 47 (1981) 649.

⁵O.Gehre, O.Gruber, H.D.Murmann, D.E.Roberts, F.Wagner, et al., Phys. Rev. Lett. 60 (1988) 1502.

⁶R.J.Fonck, R.Howell, K.Jaehnig, et al., Phys. Rev. Lett. 63 (1989) 520.

⁷G.A.Hallock, J.Mathew, W.C.Jennings and R.L.Hickok, Phys. Rev. Lett. 56 (1986) 1248.

⁸G.A.Hallock, A.J.Wootton and R.L.Hickok, Phys. Rev. Lett. 59 (1987) 1301.

- ⁹K.A.Razumova, Plasma Physics and Controlled Fusion 26 (1984) 37.
- ¹⁰H.Wobig, H.Maassberg, H.Renner, W VII-TEAM, ECRH GROUP, NI GROUP in Plasma Physics and Controlled Nuclear Fusion Research (Proc. 11th Int. Conf., Kyoto, 1986) Vol 2 (1987) 369.
- ¹¹K.Kondo, H.Zushi, H.Nakamura, et al., Rev. Sci. Instrum. 59 (1988) 1533.
- ¹²K.H.Burrell R.J.Groebner, H.St.John, R.P.Seraydarian Nucl. Fusion 28 (1988) 3.
- ¹³A.Kallenbach, H.M.Mayer, K.Brau, G.Fussmann, et al., in Controlled Fusion and Plasma Physics (Proc. 16th Europ. Conf., Venice 1989) Part I, 175.
- ¹⁴H.Stix, Phys. Fluids 16 (1973) 1260.
- ¹⁵K.Brau, M.Bitter, R.J.Goldston, D.Manos, K.McGuire and S.Suckewer, Nucl. Fusion 23 (1983) 1643.
- ¹⁶R.D.Benjamin, J.L.Terry, H.W.Moos, Rev. Sci. Instrum. 57 (1986) 2021.
- ¹⁷F.L.Hinton and R.D.Hazeltine, Rev. Mod. Phys, 48 (1976) 239.
- ¹⁸K.Ida and S.Hidekuma, Rev. Sci. Instrum. 60 (1989) 867.
- ¹⁹S.Morita, et al., in Controlled Fusion and Plasma Heating, (Proc. 14th Europ. Conf., Madrid, 1987) Vol. III, European Physical Society (1987) 874.
- ²⁰K.Kawahata, T.Tesuka, J.Fujita, M.Nagatsu, H.Ohnishi, S.Okajima and T.Iwasaki, Int. J. IR and MM Waves 9 (1988) 655.
- ²¹K.T.Tsang and E.A.Frieman Phys. Fluids, 19 (1976) 752.
- ²²K.C.Shaing and J.D.Callen Phys. Fluids, 25 (1982) 1012.
- ²³K.Kawahata, et al., in Plasma Physics and Controlled Nuclear Fusion Research (Proc. 12th Int. Conf., Nice, 1988) IAEA-CN-50/5-3-1.
- ²⁴K.Ida, T.Amano, K.Kawahata, O.Kaneko, Research Report IPPJ-896 (Inst. of

Plasma Phys. Nagoya Univ. 1988).

Figure caption

Fig.1 Radial profile of (a) toroidal rotation velocity (b) ion temperature (c) electron density for NBI and for NBI + ICRF heated plasma.

Fig.2 (a) Radial electric field and (b) space plasma potential distribution. The dashed lines stand for the estimations by neoclassical ripple transport theory, while the solid lines stand for the estimations from the model of particle fluxes .

Fig.3 Central plasma potential as a function of the central ion temperature for NBI and ICRF heated plasma. The closed circles denote co-injection case, while closed squares denote counter-injection case. The dashed line stands for the estimation by neoclassical ripple transport theory, while the solid line stands for the estimation from the model of particle fluxes.

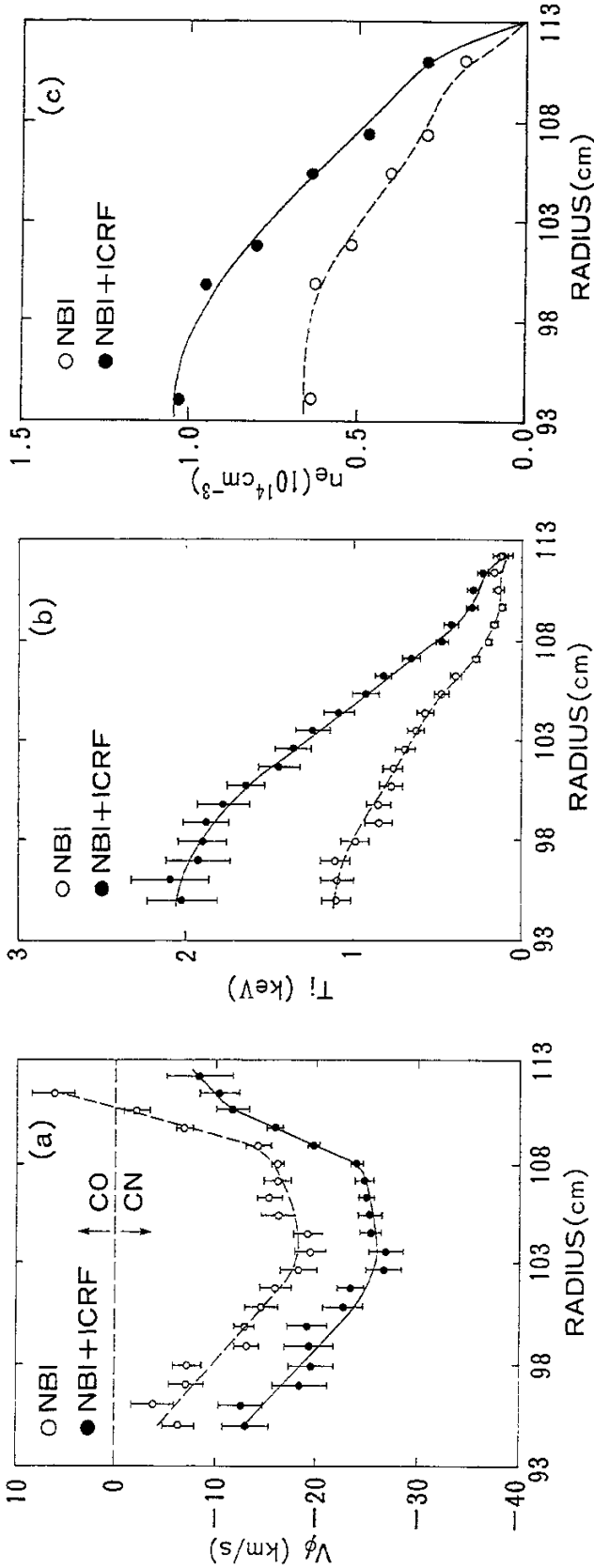


Fig. 1

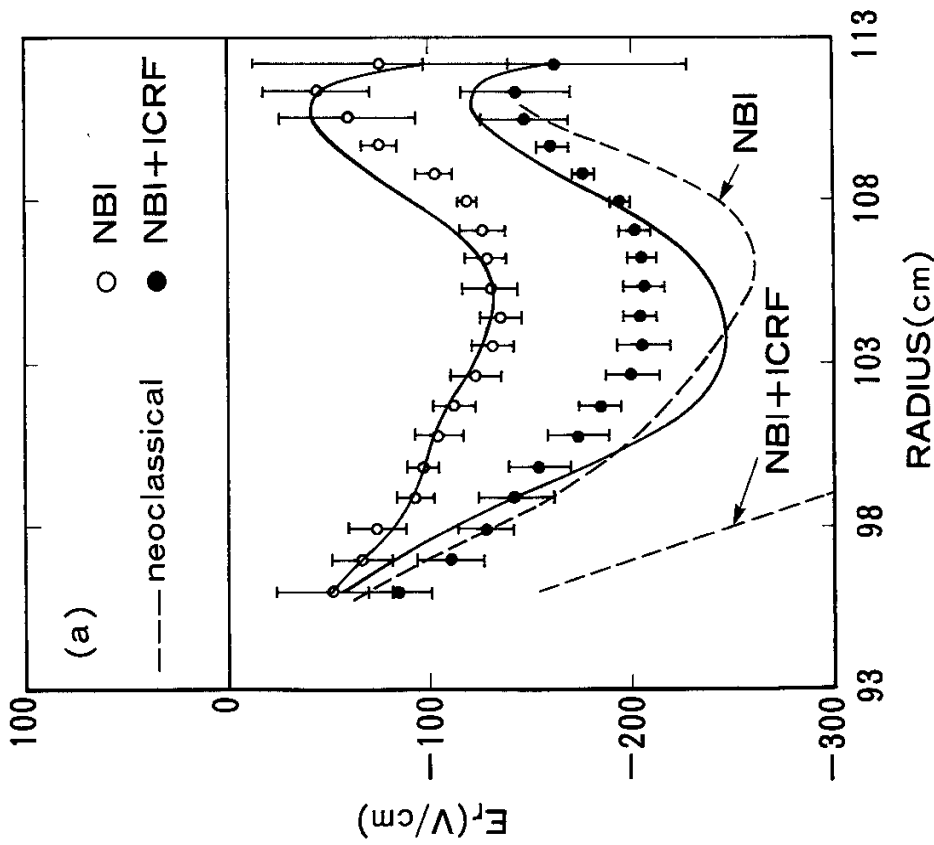
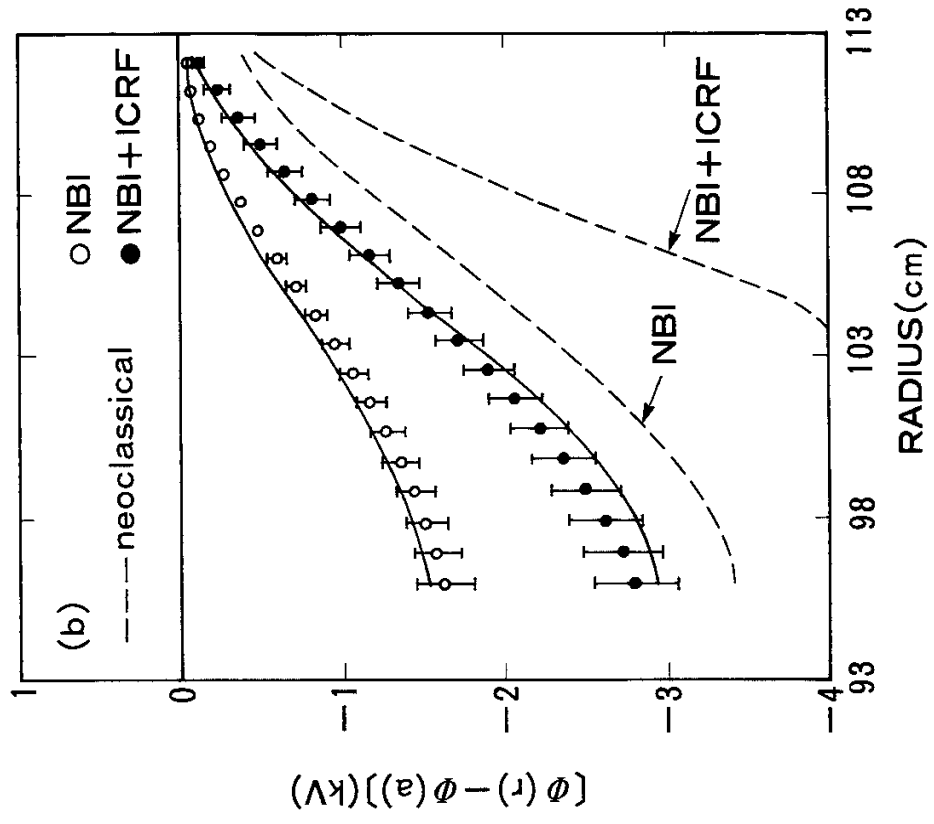


Fig.2

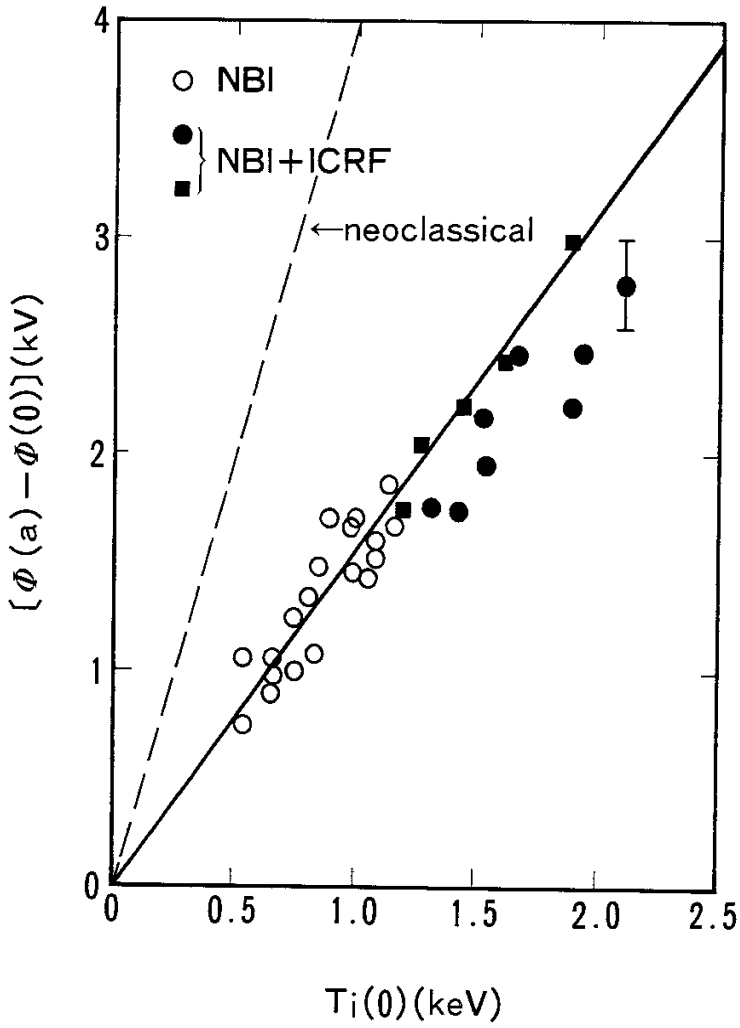


Fig.3